Journal of Photochemistry and Photobiology A: Chemistry 202 (2009) 142–153

Contents lists available at ScienceDirect

Journal of Photochemistry and Photobiology A: Chemistry

journal homepage: www.elsevier.com/locate/jphotochem

Treatment of azo dye production wastewaters using Photo-Fenton-like advanced oxidation processes: Optimization by response surface methodology

Idil Arslan-Alaton*, Gokce Tureli, Tugba Olmez-Hanci

Istanbul Technical University, Faculty of Civil Engineering, Department of Environmental Engineering, 34469 Maslak, Istanbul, Turkey

ARTICLE INFO

Article history:
Received 11 July 2008
Received in revised form 6 November 2008
Accepted 29 November 2008
Available online 11 December 2008

Keywords:
Azo dye production wastewater
Photo-Fenton-like treatment
Process optimization
Response surface methodology (RSM)
•OH scavenger Cl^-

ABSTRACT

Treatability of synthetic azo dye production wastewaters from Acid Blue 193 and Reactive Black 39 production and real Reactive Black 39 production effluent via Photo-Fenton-like process was investigated. Response surface methodology was employed to assess individual and interactive effects of critical process parameters (Fe^{3+}, H_2O_2 concentrations; initial chemical oxygen demand (COD) and reaction time) on treatment performance in terms of color, COD and total organic carbon (TOC) removal efficiencies. Optimized reaction conditions for synthetic AB 193 production wastewater were established as Fe^{3+} = 1.5 mM; H_2O_2 = 35 mM for CODs ≤ 200 mg/L and a reaction time of 45 min. Under these conditions, 98% color, 78% COD and 59% TOC removals were experimentally obtained and fitted the model predictions well. The same model also described the treatment of synthetic Reactive Black 39 production wastewater satisfactorily. Experimentally achieved removals were considerably lower than model predictions for real Reactive Black 39 production effluent due to its high chloride content.

1. Introduction

Dye manufacturing wastewater generally contains residual dyestuffs, dye intermediates as well as unreacted raw materials such as aromatic amines with alkyl-, halogen-, nitro-, hydroxyl-, sulfonic acid-substituents, and inorganic sodium salts [1]. Waste streams being variable in composition and strength are generated at different stages of the dye manufacturing process. The effluent is generally characterized by its high chemical oxygen demand (COD), total dissolved solids (TDS) content, intense color and low biodegradability, implying the presence of recalcitrant organic matter [1,2]. Dyes and dye intermediates can undergo reductive processes in the aquatic environment, resulting in the formation of potentially carcinogenic/mutagenic compounds (e.g. naphthylamines, substituted phenylamines, benzidine analogues) and cause abnormal coloration [3]. Dye manufacturing effluent may also contain free and complexed, toxic heavy metals (i.e. cobalt, chromium and copper) that result from the production of metal-complex azo dyes. Since the environmental characteristics of dye manufacturing wastewater are not suitable for the application of biological treatment technologies, the conventional treatment of dye production wastewater involves adsorption, coagulation and precipitation. However, these phase-transfer methods are not always effective in the removal of polar and hence very water soluble dyes from the effluent. Besides, both treatment processes have major drawbacks such as disposal/treatment of the created chemical sludge or regeneration/replacement of the spent adsorbent [4]. Oxidative treatment with chlorine or ozone is another plausible alternative for dealing with dye manufacturing effluents. Although chlorine is a powerful oxidant, chlorination has the inherent disadvantage of generating organic halogenated byproducts and it application is currently being ruled out. On the other hand, ozonation combined with coagulation is being employed in real practice, providing efficient color but low organic carbon removal. A major drawback of ozonation is its high electrical energy requirement [5,6].

Recent studies indicated that so-called advanced oxidation processes (AOPs) might be a good alternative for treating recalcitrant and/or toxic pollutants [7]. AOPs involve the production of strongly oxidizing agents, mainly hydroxyl radicals (•OH) that react rapidly and almost non-selectively with most inorganic and organic compounds including biologically difficult-to-degrade azo dyes and dye intermediates [8]. Among the AOPs, ozonation combined with H_2O_2, UV-C or both, H_2O_2/UV-C oxidation, Fenton and Photo-Fenton treatment, heterogeneous photocatalytic processes

Abbreviations: ANOVA, Analysis of Variance; CCD, Central Composite Design; COD, chemical oxygen demand (mg/L); TOC, total organic carbon (mg/L); k, reaction rate constant ($time^{-1}$); K, equilibrium constant; TDS, total dissolved solids (mg/L); λ_{max}, the wavelength of the maximum absorption band (nm); R^2, correlation coefficient; RSM, response surface methodology; DF, degrees of freedom; Prob > F, probability value; F-value, Fisher variation ratio; COD_o, initial chemical oxygen demand (mg/L); pH_o, initial pH; $[Fe^{3+}]_o$, initial ferric ion concentration (mmol/L); $[Fe^{3+}]$, ferric ion concentration (mmol/L); $[H_2O_2]$, hydrogen peroxide concentration (mmol/L); $[H_2O_2]_o$, initial hydrogen peroxide concentration (mmol/L); t_r, reaction time (min); ϕ, quantum yield for photoreduction of Fe^{3+} to Fe^{2+}; •OH, hydroxyl radical; HO_2•, hydroperoxyl radical; •OH, hydroxyl radical; HO_2•, hydroperoxyl radical; Cl•, chloride radical; Cl_2•$^-$, chlorine radical.

* Corresponding author. Tel.: +90 212 285 37 86; fax: +90 212 285 65 45.
E-mail address: arslanid@itu.edu.tr (I. Arslan-Alaton).

1010-6030/$ – see front matter © 2008 Elsevier B.V. All rights reserved.
doi:10.1016/j.jphotochem.2008.11.019

mediated by the semiconductors TiO_2, ZnO and CdS, electrochemical processes, catalytic ultrasound (sonolysis), wet air oxidation and supercritical water oxidation have been reported in the scientific literature as effective means for the treatment of colored aromatics such as textile azo dyes [9–12]. The advanced oxidation of textile dyes and dyehouse effluent with Fenton and Photo-Fenton processes have recently received great attention because of their high efficiency in decolorization, ease of operation and relatively low operating costs [13]. However, only few studies are available in scientific literature dealing with the application of AOPs to treat dye manufacturing wastewater [4,14,15] although the application of AOPs to this type of wastewater is definitely more attractive than treating dyehouse effluent, owing to the low volume and high recalcitrance of dye manufacturing wastewater. In fact, some dye manufacturing effluent streams (i.e. wastewater created during reactor rinsing as well as dye separation/purification-reverse osmosis-outflows) are quite suitable for photochemical oxidation due to their relatively low volume and lower pollution load (COD ≤ 500 mg/L) despite their intense color.

Fenton's reagent (Fe^{2+}/H_2O_2) involves the catalytic decomposition of hydrogen peroxide by ferrous ions under acidic pH conditions [16–18], whereas Photo-Fenton ($Fe^{2+}/H_2O_2/UV$) and Photo-Fenton-like ($Fe^{3+}/H_2O_2/UV$) processes are its "photochemically enhanced version" [19,20]. Fenton as well as Photo-Fenton type processes are favored by acidic pH conditions (2–5) with a distinct optimum range of pH 2.8–3.0 [20]. However, as the solution pH is higher in many cases, the necessity to acidify the reaction medium limits the applicability of the Fenton process in practice. Besides this strict limitation, iron hydroxide sludge is produced at the end of the reaction which needs further treatment and disposal as solid waste [21]. The application of UV-C and even UV-A (near-UV) radiation during the Fenton process causes a dramatic increase in the •OH formation efficiency thus enabling the use of lower iron catalyst concentrations [22]:

$$\mathrm{Fe(III)OH^{2+}} + h\upsilon \rightarrow \mathrm{Fe^{2+}} + {}^{\bullet}\mathrm{OH} \text{ with } \phi \text{ at } 347\,\mathrm{nm} = 0.2 \text{ and } k = 0.0012\,\mathrm{s^{-1}} \quad (1)$$

The above reaction results in the continuous support of Fe^{2+} iron for the direct Fenton reaction, thus minimizing the required Fe^{2+} concentration, enhancing the catalytic oxidation cycle and providing additional •OH. The photoreduction of ferric iron complexes is a strong function of the irradiation wavelength (e.g. the emission band of the UV light source) as well as reaction pH [22,23].

Using ferric iron was preferred in this experimental study considering our previous experimental findings [9] reporting that hydrogen peroxide consumption is more efficient during the Photo-Fenton-like process as compared with the Photo-Fenton process since initially there is no ferrous iron in the reaction solution and its formation depends on the photoreduction of Fe^{3+}-complexes and the dark Fenton-like process;

$$\mathrm{Fe^{3+}} + \mathrm{H_2O_2} \rightarrow \mathrm{Fe^{2+}} + \mathrm{H^+} + \mathrm{HO_2}^{\bullet} \quad (2)$$

Since Photo-Fenton-like oxidation is affected by numerous process parameters such as iron (catalyst) concentration, hydrogen peroxide (oxidant) concentration, reaction pH and initial pollutant concentration (COD and TOC); working conditions are case-specific and need to be carefully optimized. The majority of recent studies concerned with the effect of these process variables on the treatment efficiency and reaction kinetics were performed using a rather one-factor-at-a-time approach, where one parameter was varied thereby keeping the others constant. However, the process parameters may involve synergistic effects, as a result of complex interactions between the process variables. Hence, the application of conventional optimization techniques is not adequate for process optimization, very time consuming, and does not necessarily allow a precise process optimization. As to overcome these drawbacks, experimental process optimization should be based on statistical design tools. In the design and statistical evaluation of experiments, response surface methodology (RSM) can be used for process optimization and prediction of the interaction between process variables, reducing the numbers and thus the time and associated costs spent for conducting these experiments [24]. RSM has already proven to be a reliable statistical tool in the investigation of chemical treatment processes [25]. RSM has been applied in numerous studies to optimize treatment of textile dyes and simulated/real dyehouse effluent [26–31]. As far as we are concerned, no scientific work has been published dealing with the application of RSM to treat azo dye manufacturing wastewater so far. The relatively low volume, neutral-to-slightly acidic pH as well as refractory organic carbon content of textile production effluent render it an ideal candidate for treatment with iron-based advanced oxidation processes.

Considering the above-mentioned facts, the present work aimed at investigating the treatability of synthetic and real azo dye production wastewaters with the Photo-Fenton-like process. RSM was applied to assess the individual and interactive effects of several operating parameters on treatment efficiency. Central Composite Design (CCD), which is the most widely used form of RSM, was employed to evaluate the effect of important process variables (irradiation time, catalyst and oxidant concentration, organic carbon content of the wastewater) on color, COD and TOC removal efficiencies. Process modeling and optimization studies focused on synthetic effluent originating from Acid Blue 193 production (reactor washing stage) and model predictions were experimentally validated. Photo-Fenton-like oxidation of synthetic Reactive Black 39 (reactor washing stage) and real Reactive Black 39 (reverse osmosis purification stage) production effluent was also performed under optimized working conditions established by the model for Acid Blue 193 production effluent. In this context, the applicability of the derived model predictions on Photo-Fenton-like treatment of several azo dye production effluents could be explored more comprehensively.

2. Materials and methods

2.1. Azo dye production wastewaters

Synthetic Acid Blue 193 (a chromium complex disazo dye; AB 193) and Reactive Black 39 (a disazo dye; RB 39) production wastewaters were prepared to simulate effluent originating from the azo dye synthesis reactor washing stages. In order to attain uniformity throughout the optimization experiments, synthetic wastewaters were prepared by dissolving the synthesized, azo dye formulations (obtained prior to their purification) supplied by a local dye manufacturing company, in distilled water. Synthetic AB 193 production effluent samples that were used throughout the optimization runs were daily prepared to attain effluent CODs of 100, 150, 200, 250 and 300 mg/L. The studied COD range was selected upon consideration of typical process and effluent conditions at textile dye manufacturing plants, while increments of 50 mg/L COD were determined according to the employed RSM. Synthetic RB 39 production wastewater was prepared to attain a COD of around 200 mg/L, so that optimum Photo-Fenton-like conditions established for the COD range 150–200 mg/L via RSM could be applied.

Real RB 39 dye production wastewater (RB 39-RO) was provided by the same company from where the raw RB 193 and RB 39 dyes were obtained. The real effluent was taken from a holding tank containing the permeate produced during reverse osmosis RB 39 purification. This effluent was diluted three times with distilled water in order to attain a COD of ≤200 mg/L. Some environmental char-

Table 1
Environmental characteristics of the synthetic and real azo dye production wastewaters.

Parameter	AB 193 (COD = 200 mg/L)	RB 39 (COD = 195 mg/L)	RB 39[a] (COD = 165 mg/L)
Absorbance, λ_{max} (cm^{-1})	3.512 at 576 nm	9.310 at 611 nm	4.792 at 611 nm
TOC (mg/L)	65	72	66
Cl^- (mg/L)	130	190	3500
pH	6.0	6.0	5.8

[a] Real effluent from reverse osmosis separation purification permeate.

acteristics of the three azo dye production effluents were given in Table 1.

2.2. Other reagents and supplies

35% (w/v) H_2O_2 (Fluka), was stored in a cool room and used as received without any dilution. The ferric iron catalyst source was prepared for daily use by dissolving $Fe(NO_3)_3{\cdot}9H_2O$ (Fluka), in distilled water to obtain a 10% (w/v) stock solution. The approximate amount of residual H_2O_2 was determined using Peroxide Quant test strips (Aldrich) and Catalase enzyme (Fluka, obtained from *Micrococcus lyseidicticus*; 1 activity unit destroys 1 μmol H_2O_2 at pH 7, 200181 AU/mL) was used to destroy unreacted H_2O_2 that may positively interfere with COD measurements. Several concentrations of HNO_3 and NaOH (Merck) solutions were prepared for pH adjustment at any stage of the experiments.

2.3. Photo-Fenton-like experiments

Photo-Fenton-like oxidation of azo dye production wastewaters were carried out in 100 mL capacity cylindrical Pyrex glass reaction vessels. UV-A irradiation was performed with a 150 W black light bulb lamp, emitting radiation between 310 and 390 nm and having a maximum emission band at 360 nm. The incident light flux of the UV-A lamp was determined as 2.6×10^{-5} Einstein/min by ferrioxalate actinometry [32]. The photoreactor was located inside a box (dimensions = 60 cm × 40 cm × 55 cm) with its three inner sides covered by mirrors enabling efficient UV-A light distribution across the reaction vessel. First, Fe^{3+} catalyst was added to the pH-adjusted reaction solution and a sample $t = 0$ was taken under continuous stirring of the vessel at 100 rpm to ensure sufficient aeration at the same time. Thereafter, the reaction solution was located under the UV-A lamp which was turned on 20 min before the start of the reaction to obtain a constant light emission. Photo-Fenton-like reaction was initiated by the addition of proper amounts of H_2O_2 oxidant. Samples were taken regularly during the course of the photochemical experiments for up to 60 min. In order to avoid changes in irradiated volume, the reaction was restarted after each sampling period. Absorbance measurements were done immediately after the samples were taken while COD and TOC measurements were conducted after pH re-adjustment to around 7.0 followed by filtration through 0.45 μm Millipore membranes to remove the formed ferric hydroxide precipitate.

2.4. Analytical procedures

All measurements were done at least in duplicate. Throughout all experimental runs, color was directly recorded on a Novespec II/Pharmacia LKB spectrophotometer at the maximum absorption bands (λ_{max} values) of synthetic AB 193 (=576 nm) and synthetic/real RB 39 production (=611 nm) wastewaters. The TOC values of all filtered samples were determined on a Shimadzu TC (total carbon) V_{PCN} carbon analyzer equipped with an autosampler. COD analyses of the synthetic azo dye production wastewaters were carried out according to ISO 6060 [33] by the closed reflux, titrimetric method, whereas the CODs of the real azo dye production effluent (the permeate of the reverse osmosis dye separation/purification stage) were determined in accordance with DIN 38 409 H 41-2 [34] by the open reflux, titrimetric method, due to its high chloride content. The pH was measured with a Thermo Orion model 520 pH-meter at any stage of the experiments. Chloride measurements were conducted according to the mercuric nitrate method as described in standard methods [35].

2.5. Experimental design, data analysis and process optimization

RSM is a statistical method being useful for the optimization of chemical reactions and/or industrial processes and widely used for experimental design [25]. Whenever multiple system variables may influence the outputs, RSM can be utilized to assess the relationship between dependent (response) and independent variables as well as to optimize the relevant processes [36].

RSM employs a low-order polynomial equation in a predetermined region of the independent variables, which are later on analyzed to locate the optimum values of independent variables to obtain the best (highest) response [37]. Process optimization by RSM is faster for gathering experimental research results than the rather conventional, time consuming one-factor-at-a-time approach [24].

In the present study, Central Composite Design (CCD), which is a widely used form of RSM was employed for the optimization of Photo-Fenton-like treatment of azo dye production wastewater. It is an ideal design tool for sequential experimentation and allows testing the lack of fit when an adequate number of experimental values are available. A four-factorial, five-level CCD consisting of 26 experimental runs was performed in the present work, including two replications at the center point. Initial Fe^{3+} and H_2O_2 concentrations, initial CODs of the wastewater and reaction time (t_r) were considered as the independent, process-specific variables, while percent color, COD and TOC removal efficiencies were considered as the dependent variables (responses). Values of the independent variables and their variation limits were determined basing on the related scientific literature as well as experimental results obtained in preliminary studies conducted with azo dye and are presented in Table 2.

Experimental data were analyzed using the trial version of Design-Expert 6.0.7 software and fitted to a second-order polynomial equation. The following function was employed to attain the interaction between the dependent and independent variables [38]:

$$Y = b_0 + \sum b_i X_i + \sum b_{ii} X_i^2 + \sum b_{ij} X_i X_j \quad (3)$$

Table 2
Experimental range and levels of independent process variables.

Process variables	Code	Real values of the coded levels				
		−2	−1	0	1	2
$[Fe^{3+}]_o$, mM	X_1	0.5	1.5	2.5	3.5	4.5
$[H_2O_2]_o$, mM	X_2	25	35	45	55	65
t_r, min	X_3	0	15	30	45	60
COD_o, mg/L	X_4	100	150	200	250	300

Table 3
Experimental design matrix and response based on experimental runs and predicted values on color, COD and TOC removals (%) proposed by CCD design.

Run	Independent variables				Response (Y, %)					
	X_1	X_2	X_3	X_4	Experimental			Predicted		
	$[Fe^{3+}]_o$ (mM)	$[H_2O_2]_o$ (mM)	t_r (min)	COD_o (mg/L)	Color	COD	TOC	Color	COD	TOC
1	1.5	55	15	250	96	45	32	89	53	32
2	2.5	45	30	200	97	78	51	97	78	51
3	2.5	65	30	200	98	78	49	100	76	44
4	2.5	45	30	100	98	73	78	100	79	73
5	2.5	45	0	200	36	49	31	60	55	34
6	3.5	55	15	150	97	78	48	90	76	51
7	3.5	35	45	250	96	78	55	99	83	56
8	4.5	45	30	200	97	83	53	100	87	54
9	3.5	55	45	250	98	84	57	100	86	56
10	3.5	55	45	150	99	80	59	100	82	61
11	1.5	35	45	250	98	74	49	100	77	51
12	1.5	55	15	150	98	70	48	90	65	47
13	1.5	55	45	250	98	63	39	100	68	46
14	1.5	35	15	150	96	73	43	89	73	49
15	3.5	55	15	250	97	81	51	89	77	50
16	2.5	25	30	200	96	81	48	100	81	47
17	2.5	45	60	200	98	83	74	83	75	65
18	3.5	35	45	150	97	83	60	99	77	65
19	0.5	45	30	200	97	77	51	100	70	45
20	3.5	35	15	250	95	76	44	87	76	44
21	2.5	45	30	200	97	78	51	97	78	51
22	2.5	45	30	300	98	81	50	100	73	49
23	1.5	35	45	150	98	80	74	100	85	74
24	1.5	35	15	250	96	64	31	89	63	30
25	3.5	35	15	150	95	76	55	88	72	48
26	1.5	55	45	150	98	76	60	100	78	66

In this equation, Y represents the predicted dependent variables (responses), X_i's are the independent variables, b_0 is the constant coefficient and b_i, b_{ii} and b_{ij} are the interaction coefficients. The quality of the fit of polynomial model was expressed by the value of correlation coefficient (R^2). The model F-value (Fisher variation ratio), probability value (Prob > F) and adequate precision are the main indicators showing the significance and adequacy of the employed model. Simultaneous consideration of multiple responses involves first of all building an appropriate response surface model and thereafter searching for a set of working conditions that optimize all responses or at least keeps them in desired ranges [25]. The optimization module in Design-Expert searches for a combination of factor levels that simultaneously satisfy the requirements placed on each of the responses. For process optimization, the desired goals for each process (independent) variable and response (dependent) should be established first. In the present study, desired goals for the responses (percent color, COD and TOC removals) were chosen as to "maximize", while process variables (initial Fe^{3+} and H_2O_2 concentrations, reaction time) were selected to be "within the range". Then, these individual goals were combined into an overall desirability function by the software for maximization to find the best local maximum [39].

3. Results and discussion

3.1. Model results for Photo-Fenton-like oxidation of synthetic Acid Blue 193 production wastewater

Synthetic AB 193 production wastewater was prepared at varying CODs and subjected to Photo-Fenton-like treatment under different conditions in accordance with the experimental runs indicated by the model. The complete 26 numbers of the experimental design matrix and responses based on experimental runs and predicted values on percent color, COD and TOC removals proposed by CCD are given in Table 3. The observed percent COD and TOC removal efficiencies varied between 45–84% and 31–78%, respectively, and the model predictions matched these experimental results satisfactorily. On the other hand, as is also evident in Table 3, percent color removal efficiencies varied between 97 and 99%, but the predicted values did not fit the experimental ones very well. Based on these results, an empirical relationship between the responses and independent variables were attained for AB 193 production effluent and expressed by the following second-order polynomial equations;

$$\begin{aligned}\text{color removal}(\%) = {} & 108.38271 - 7.52042 \cdot Fe^{3+} - 0.90554 H_2O_2 \\ & + 2.11956 \cdot t_r - 0.19504 \cdot COD \\ & + 1.20729 \cdot (Fe^{3+})^2 + 0.010723 \cdot (H_2O_2)^2 \\ & - 0.028240 \cdot (t_r)^2 + 5.11417 \cdot 10^{-4} \cdot COD^2 \\ & + 0.034125 \cdot Fe^{3+} \cdot H_2O_2 - 8.33333 \\ & \times 10^{-4} \cdot Fe^{3+} \cdot t_r - 1.1 \times 10^{-3} \cdot Fe^{3+} \cdot COD \\ & - 1.15 \times 10^{-3} \cdot H_2O_2 \cdot t_r - 2.65 \times 10^{-4} \cdot H_2O_2 \\ & \cdot COD + 4.5 \times 10^{-5} \cdot t_r \cdot COD \end{aligned} \quad (4)$$

$$\begin{aligned}\text{COD removal}(\%) = {} & 109.71042 - 20.15354 \cdot Fe^{3+} - 0.86098 \cdot H_2O_2 \\ & + 1.25633 \cdot t_r - 0.10762 \cdot COD + 0.20365 \\ & \cdot (Fe^{3+})^2 + 2.32396 \times 10^{-3} \cdot (H_2O_2)^2 - 0.0142 \\ & \cdot (t_r)^2 - 1.68542 \times 10^{-4} \cdot COD^2 + 0.29356 \\ & \cdot Fe^{3+} \cdot H_2O_2 - 0.11279 \cdot Fe^{3+} \cdot t_r + 0.068163 \\ & \cdot Fe^{3+} \cdot COD + 7.625 \times 10^{-4} \cdot H_2O_2 \cdot t_r \\ & - 1.18625 \times 10^{-3} \cdot H_2O_2 \cdot COD + 8.92500 \\ & \times 10^{-4} \cdot t_r \cdot COD \end{aligned} \quad (5)$$

Table 4
ANOVA results of the quadratic polynomial model for photo-Fenton-like treatment of synthetic AB 193 production wastewater.

	Source	Sum of squares	Degrees of freedom	Mean square	*F*-value	Prob > *F*
Color removal	Model	2173.04	14	155.22	1.21	0.3807
	Residual	1410.88	11	128.26		
	Lack of fit	1410.88	10	141.09		
	Pure error	0.00	1	0.00		
	R^2 = 0.6063, adequate precision = 4.920					
COD removal	Model	1811.46	14	129.39	2.74	0.050
	Residual	520.16	11	47.29		
	Lack of fit	520.16	10	52.02		
	Pure error	0.00	1	0.00		
	R^2 = 0.7769, adequate precision = 6.565					
TOC removal	Model	3099.00	14	221.36	6.70	0.0016
	Residual	363.58	11	33.05		
	Lack of fit	363.58	10	36.36		
	Pure error	0.00	1	0.00		
	R^2 = 0.8950, adequate precision = 10.179					

$$\begin{aligned}\text{TOC removal}\,(\%) = {} & 96.61344 - 10.63333\,Fe^{3+} + 0.84571 \cdot H_2O_2 \\ & + 1.78315 \cdot t_r - 0.74934 \cdot \text{COD} - 0.44531 \\ & \cdot (Fe^{3+})^2 - 0.013791 \cdot (H_2O_2)^2 - 1.85694 \\ & \times 10^{-3} \cdot (t_r)^2 + 1.00438 \times 10^{-3} \cdot \text{COD}^2 \\ & + 0.10631 \cdot Fe^{3+} \cdot H_2O_2 - 0.14596 \cdot Fe^{3+} \cdot t_r \\ & + 0.073763 \cdot Fe^{3+} \cdot \text{COD} - 0.010996 \cdot H_2O_2 \cdot t_r \\ & + 1.95625 \times 10^{-3} \cdot H_2O_2 \cdot \text{COD} - 1.47917 \\ & \times 10^{-3} \cdot t_r \cdot \text{COD} \end{aligned} \quad (6)$$

The model adequacy check is an integral part of the data analysis as the approximating model functions would give poor or misleading results if the fit is inadequate [30]. Table 4 shows the Analysis of Variance (ANOVA) results of the established model for percent color, COD and TOC removals. The mean squares were obtained by dividing the sum of squares of each of the two sources of variation, the model and the error (residual) variance, by the respective degrees of freedom (DF). The model *F*-value was calculated by dividing the model mean square by residual mean square.

Values of Prob > *F* less than 0.0500 imply that the model is significant, whereas the values greater than 0.1000 are usually considered as insignificant. Prob > *F* values of 0.0500 and 0.0016 denote the employed models are significant for percent COD and TOC removals, respectively. On the other hand, the model *F*-value (1.2100) and the high Prob > *F* value (0.3807) obtained for percent color removals reveal that the model is insignificant for the color removal response; this is not surprising, since color abatement occurs promptly (within seconds) under all experimental conditions. Hence, it is quite difficult to model color removal based on the same time intervals set for COD and TOC removals because nearly complete decolorization could be achieved at these reaction times.

The R^2 value of the response variables followed the order of $R^2_{(TOC)} > R^2_{(COD)} > R^2_{(color)}$. The highest R^2 obtained for TOC removal efficiency denotes that 89.5% of the total variation could be represented by the established model expressing a satisfactory quadratic fit. However, in terms of color removal, only around 60% of the total variation could be explained by the model (R^2 = 0.6063). The adequate precision ratios of 4.920, 6.565 and 10.179 derived for percent color, COD and TOC removals, respectively, indicate an adequate signal for all response variables. Considering the above explained ANOVA test results, the model application explained the reaction quite well and can be employed to navigate the design space at least in terms of COD and TOC removal efficiencies.

3.2. Response surface and contour plots for Photo-Fenton-like treatment of synthetic Acid Blue 193 production wastewater

The three-dimensional (3D) response surface and two-dimensional (2D) contour plots of the model-predicted responses, while two variables kept at constant and the others varying within the experimental ranges, were obtained by the Design-Expert software and utilized to assess the interactive relationships between the process variables and treatment outputs for Photo-Fenton-like treatment of AB 193 production wastewater. In order to save space, only the most interesting and informative 3D and 2D plots were presented below.

3.2.1. Effect of Fe^{3+} concentration and initial COD on color removal

Percent color removal efficiencies obtained as a function of Fe^{3+} catalyst concentration and initial COD of synthetic AB 193 production wastewater was depicted in Fig. 1(a) and (b) as 2D and 3D plots, respectively. As aforementioned, high removal efficiencies (97–99%) were obtained under all working conditions, implying that changes in the process variables of Fe^{3+} concentration and initial COD within the specified range do not have a significant impact on color removals.

3.2.2. Effect of Fe^{3+} concentration and initial COD on COD removal

Fig. 2(a) and (b) shows the two- and three-dimensional interactions of initial Fe^{3+} concentration and initial effluent CODs in terms of percent COD removals, respectively. When the initial COD of the effluent was around 150 mg/L, at least 83% COD removal was obtained even with 1.5 mM Fe^{3+} in the presence of 35 mM H_2O_2 and a reaction time of 45 min. An increase in the applied Fe^{3+} concentration significantly retarded the COD removals at CODs ≤ 200 mg/L, which may be attributed to the free radical scavenging effect of excessive ("overdosed") Fe^{3+}/Fe^{2+} concentrations [40];

$$Fe^{2+} + {}^{\bullet}OH \rightarrow Fe^{3+} + OH^-, \qquad k = 3.0 \times 10^8\ M^{-1}\ s^{-1} \quad (7)$$

A decrease in the available Fe^{2+} concentration produced via photoreduction of $Fe(OH)_2{}^+$ complexes will also inhibit the direct Fenton reaction. Negative effects of excessive Fe^{2+} concentration on treatment efficiency was also reported by Giroto et al. [41], who investigated Photo-Fenton oxidation of polyvinyl alcohol using an empirical model based on neural networks.

On the other hand, as is evident from the same figure, an increase in Fe^{3+} concentration improved the COD removal efficiency at higher organic carbon loads (COD > 200 mg/L), obviously implying that the interactive effects of the Fenton reagents depend on the amount of organic matter to be oxidized. According to our kinetic

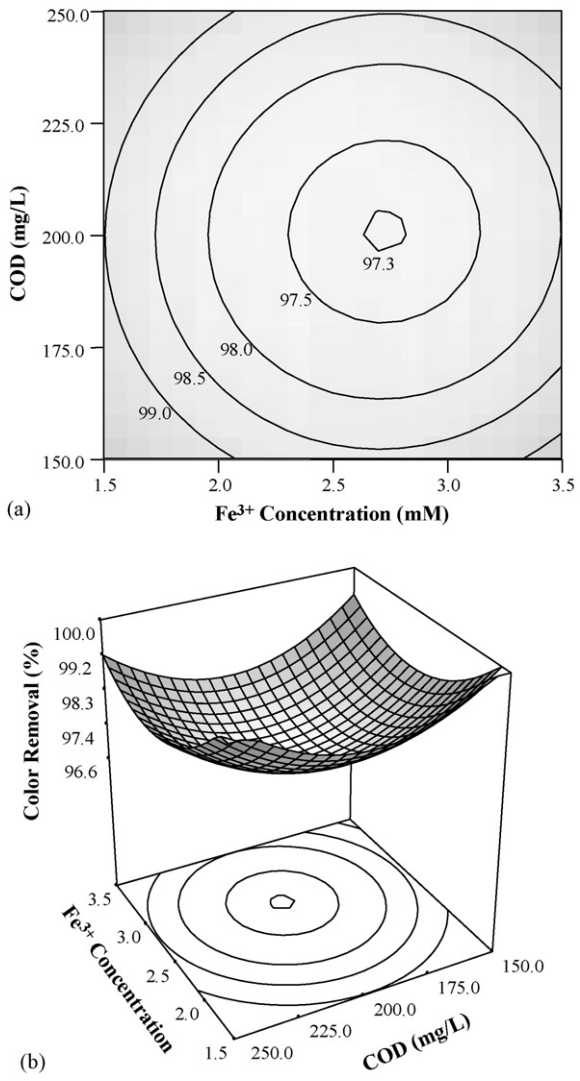

Fig. 1. Contour (a) and response surface (b) plots for percent color removal from synthetic AB 193 production wastewater as a function of initial Fe^{3+} concentration and CODs (t_r = 45 min; initial H_2O_2 concentration = 35 mM).

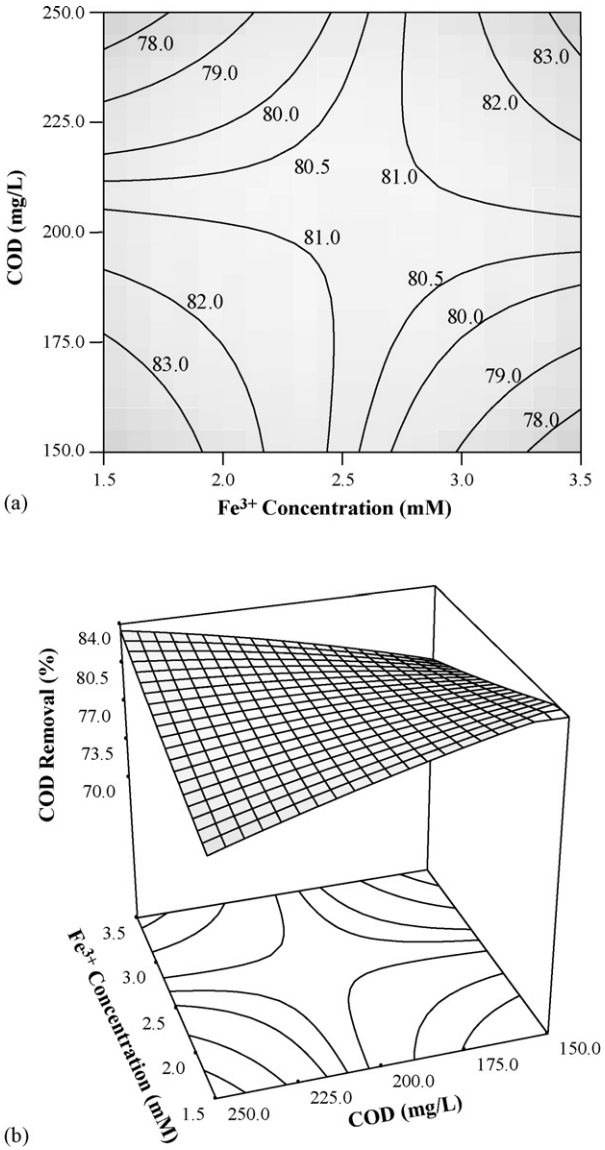

Fig. 2. Contour (a) and response surface (b) plots for percent COD removal from synthetic AB 193 production wastewater as a function of initial Fe^{3+} concentration and CODs (t_r = 45 min; initial H_2O_2 concentration = 35 mM).

model, the applied Fe^{3+} concentration should be elevated to 3.5 mM to maintain the same COD removal efficiency for initial effluent CODs of 250 mg/L.

3.2.3. *Effect of Fe^{3+} concentration and initial COD on TOC removal*

Fig. 3 displays the 2D (a) and 3D (b) plots for percent TOC removal efficiencies as a function of initial Fe^{3+} concentration and effluent initial COD (at a fixed H_2O_2 concentration of 35 mM and t_r = 45 min). As it is clear from the response contour and surface plots, TOC removal had its peak value while both of the process variables were kept at minimum. As expected, increasing the effluent COD from 150 to 250 mg/L resulted in a dramatic decrease in percent TOC removals from 70 to 54%, indicating that the treatment efficiency is strong function of the effluent's initial organic carbon content.

Generally speaking, pseudo-first order kinetics has been applied to describe pollutant abatements for advanced oxidation processes, provided that sufficient amounts of reagents are available in the reaction medium. When these conditions are satisfied, an increase in oxidation rate and efficiency is expected with increasing pollutant concentration (COD and TOC). However in former-related studies it was demonstrated that treatment efficiencies were reduced upon increasing the initial pollutant concentration [42] emphasizing that at least one of the reactant was not available in sufficient amounts. As can be seen from Fig. 3(a) and (b), mineralization of synthetic AB 193 production wastewater could globally not be represented by first-order abatement kinetics, probably due to the rate-limiting concentration of H_2O_2. At lower initial effluent CODs (<200 mg/L), TOC removals decreased with increasing Fe^{3+} concentration due to the aforementioned $^{\bullet}OH$ scavenging impact. However, the inhibitory effect of increasing Fe^{3+} concentration on TOC removal rate was less significant than its effect on percent COD removals.

3.2.4. *Effect of H_2O_2 concentration and initial COD on color removal*

Fig. 4(a) and (b) illustrates the effect of H_2O_2 concentration and initial COD upon color removals for Fe^{3+} = 1.5 mM and t_r = 45 min. As is obvious from Fig. 4, at least 98% color removal was obtained under all experimental conditions.

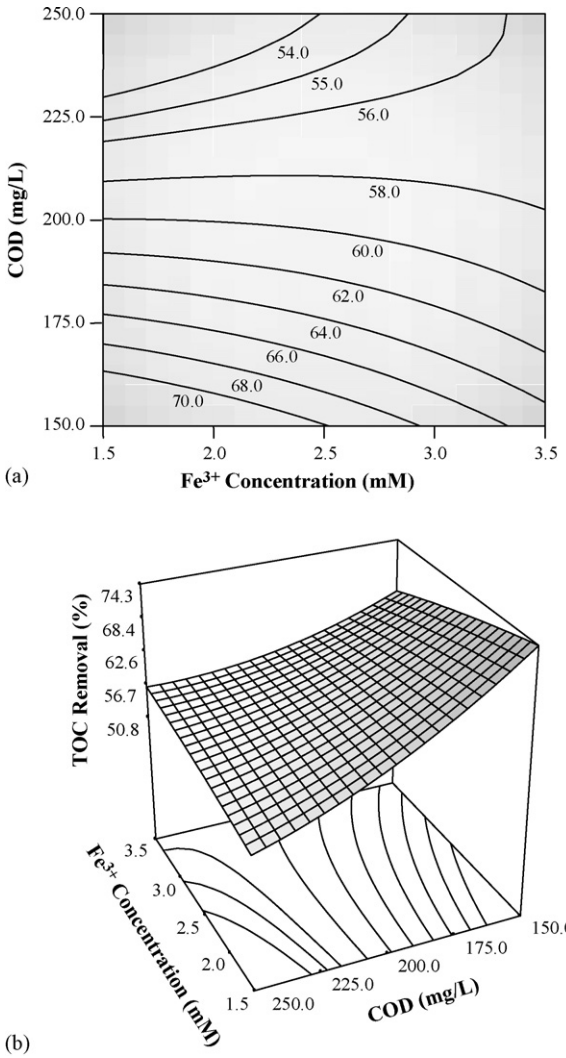

Fig. 3. Contour (a) and response surface (b) plots for percent TOC removal from synthetic AB 193 production wastewater as a function of initial Fe^{3+} concentration and CODs (t_r = 45 min; initial H_2O_2 concentration = 35 mM).

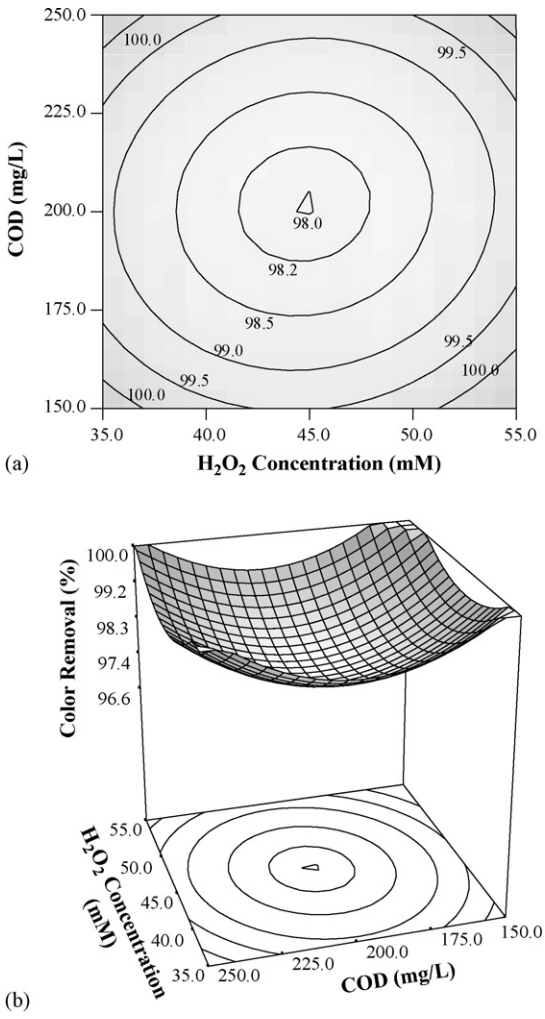

Fig. 4. Contour (a) and response surface (b) plots for percent color removal from synthetic AB 193 production wastewater as a function of initial H_2O_2 concentration and CODs (t_r = 45 min; initial Fe^{3+} concentration = 1.5 mM).

3.2.5. Effect of H_2O_2 concentration and initial COD on COD removal

Fig. 5 presents the contour (a) and response surface (b) plots as an estimate of percent COD removals as a function of the two process variables H_2O_2 concentration and initial effluent COD (Fe^{3+} = 1.5 mM; t_r = 45 min), respectively. As can be understood from Fig. 5, increasing the initial H_2O_2 concentration had a negative effect on COD removal at all selected initial CODs revealing that a concentration of 35 mM H_2O_2 was by far sufficient for the partial oxidation of synthetic AB 193 production effluent in the presence of 1.5 mM Fe^{3+}. The reduction in treatment efficiency with increasing H_2O_2 concentration was probably due to the inhibitory (free radical scavenging) effect of excessive H_2O_2 which can be expressed by the following reaction [43];

$$H_2O_2 + {}^{\bullet}OH \rightarrow H_2O + HO_2{}^{\bullet}, \qquad k = 2.7 \times 10^7\ M^{-1}\ s^{-1} \tag{8}$$

On the other hand, when a higher Fe^{3+} concentration was available; COD removals increased with increasing H_2O_2 concentration reaching their maximum values (83%) when both of the reactants were kept at their highest studied concentrations. For instance, a COD removal of ≤80% is desired, using low concentrations of both Fenton reagents might be an attractive option from both environmental and economical points of view. However, if higher COD removal efficiencies are desired (>80%), the Fe^{3+} and H_2O_2 concentrations should be elevated to 3 and 50 mM, respectively, speaking for a specific, critical "Fe^{3+}:H_2O_2" range that should be determined for each treatment case in order to achieve maximum COD removal. Selecting a pollutant specific optimum ratio between H_2O_2 and Fe^{2+}/Fe^{3+} is important in Fe-based AOPs, since •OH-scavenging reactions decreasing the oxidation efficiency occur in the presence of an excess of one of the two reagents [40].

Again, increasing the initial COD of AB 193 production wastewater led to a significant reduction in treatment efficiencies; COD removal was below 70% for an initial COD of 250 mg/L (H_2O_2 concentration = 35 mM).

3.2.6. Effect of H_2O_2 concentration and initial COD on TOC removal

Fig. 6 shows the response contour (a) and surface plots (b) for TOC removal as a function of H_2O_2 concentrations and initial effluent CODs for t_r = 45 min and Fe^{3+} = 1.5 mM. As is clear from Fig. 6, the highest TOC removal (72%) occurred when as in the case of COD removal, both of the independent parameters (H_2O_2 and initial COD) were kept at their minimum. A considerable decrease in TOC removal efficiency was observed upon elevating effluent COD at all initial H_2O_2 concentrations indicating that pseudo-first order kinetics are definitely not applicable to describe

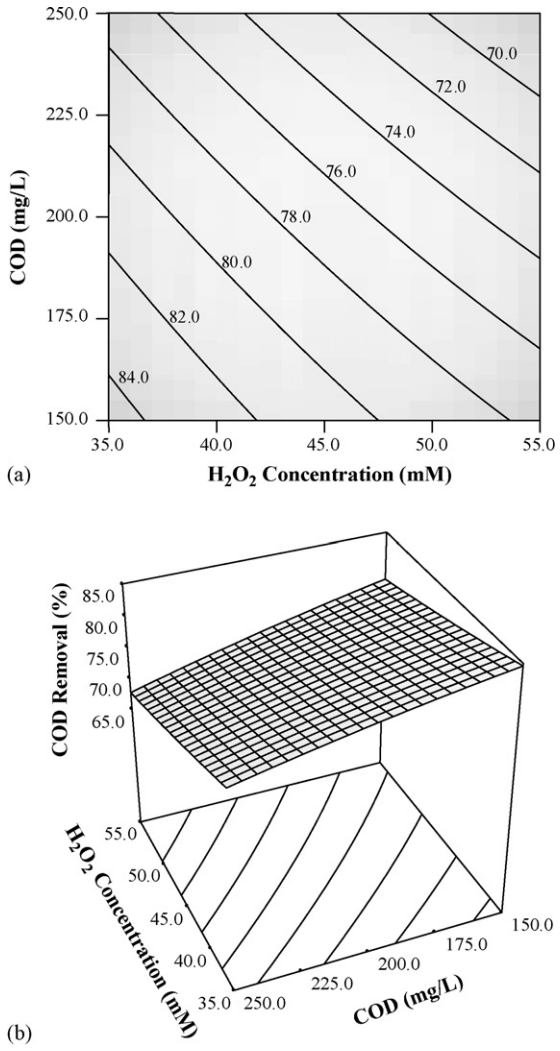

Fig. 5. Contour (a) and response surface (b) plots for percent COD removal from synthetic AB 193 production wastewater as a function of initial H_2O_2 concentration and CODs (t_r = 45 min; initial Fe^{3+} concentration = 1.5 mM).

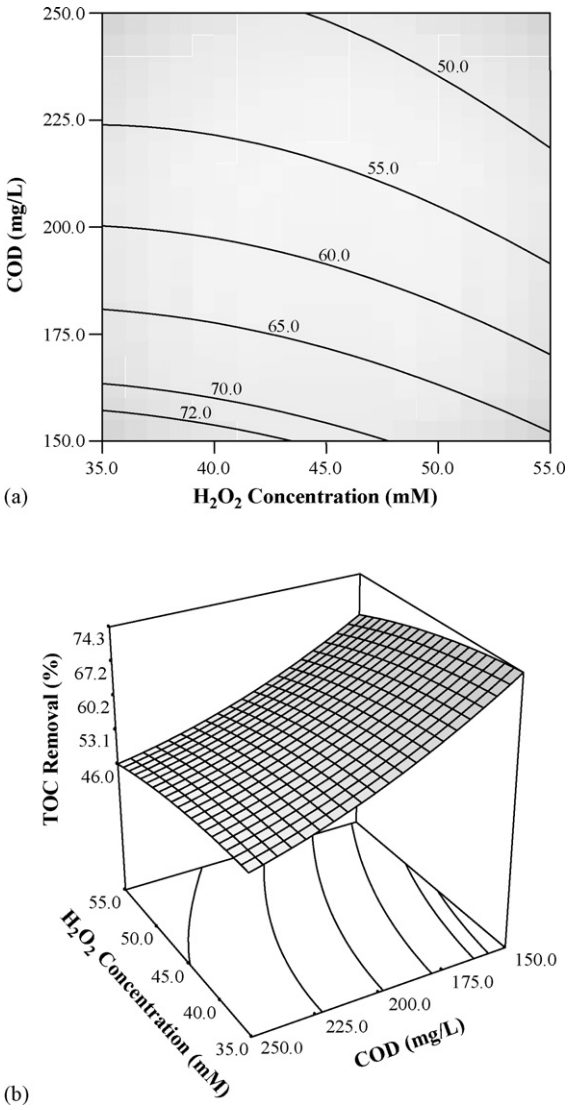

Fig. 6. Contour (a) and response surface (b) plots for percent TOC removal from synthetic AB 193 production wastewater as a function of initial H_2O_2 concentration and CODs (t_r = 45 min; initial Fe^{3+} concentration = 1.5 mM).

COD and TOC removals from AB 193 production wastewater via Photo-Fenton-like treatment, speculatively due to the rate-limiting Fe^{3+} concentration (1.5 mM). As is also evident from the figure, increasing the H_2O_2 concentration also reduced TOC removal efficiencies. However, its effect on TOC removal was less significant relative to the process variable "initial effluent COD".

3.3. Optimization of Photo-Fenton-like treatment of synthetic Acid Blue 193 production wastewater

In case of multiple responses, RSM sets forth a set of specific working conditions that in some sense maximizes all responses or at least keeps them in the desired ranges [25]. In the present study, the desired goals in terms of color, COD and TOC removal efficiencies were defined as "maximize" to achieve highest treatment performance, while the process variables Fe^{3+}, H_2O_2 concentrations and t_r were selected to be "in the range" without consideration of operating (chemicals and electrical energy) costs. Accordingly, the optimum working conditions and respective percent removal efficiencies were established for varying initial effluent CODs (local optimum values). Results were presented in Table 5.

As can be seen from Table 5, for an initial effluent COD of 200 mg/L, the model predicts 99% color, 81% COD and 60% TOC removals under optimized working conditions (1.5 mM Fe^{3+}; 35 mM H_2O_2; t_r = 45 min). Table 5 also indicates that optimum conditions for 200 mg/L COD were found identical to those predicted in case of 150 mg/L COD. When the initial COD of the effluent increased to 250 mg/L, both Fe^{3+} and H_2O_2 concentration also needed to

Table 5
Optimum working conditions established for Photo-Fenton-like treatment of synthetic AB 193 production wastewater according to RSM at varying effluent CODs.

COD_o (mg/L)	$[Fe^{3+}]_o$ (mM)	$[H_2O_2]_o$ (mM)	t_r (min)	Color removal (%)	COD removal (%)	TOC removal (%)	Desirability factor
150	1.5	35	45	100	85	74	0.98
200	1.5	35	45	99	81	60	0.84
250	3.5	44	45	99	84	57	0.83

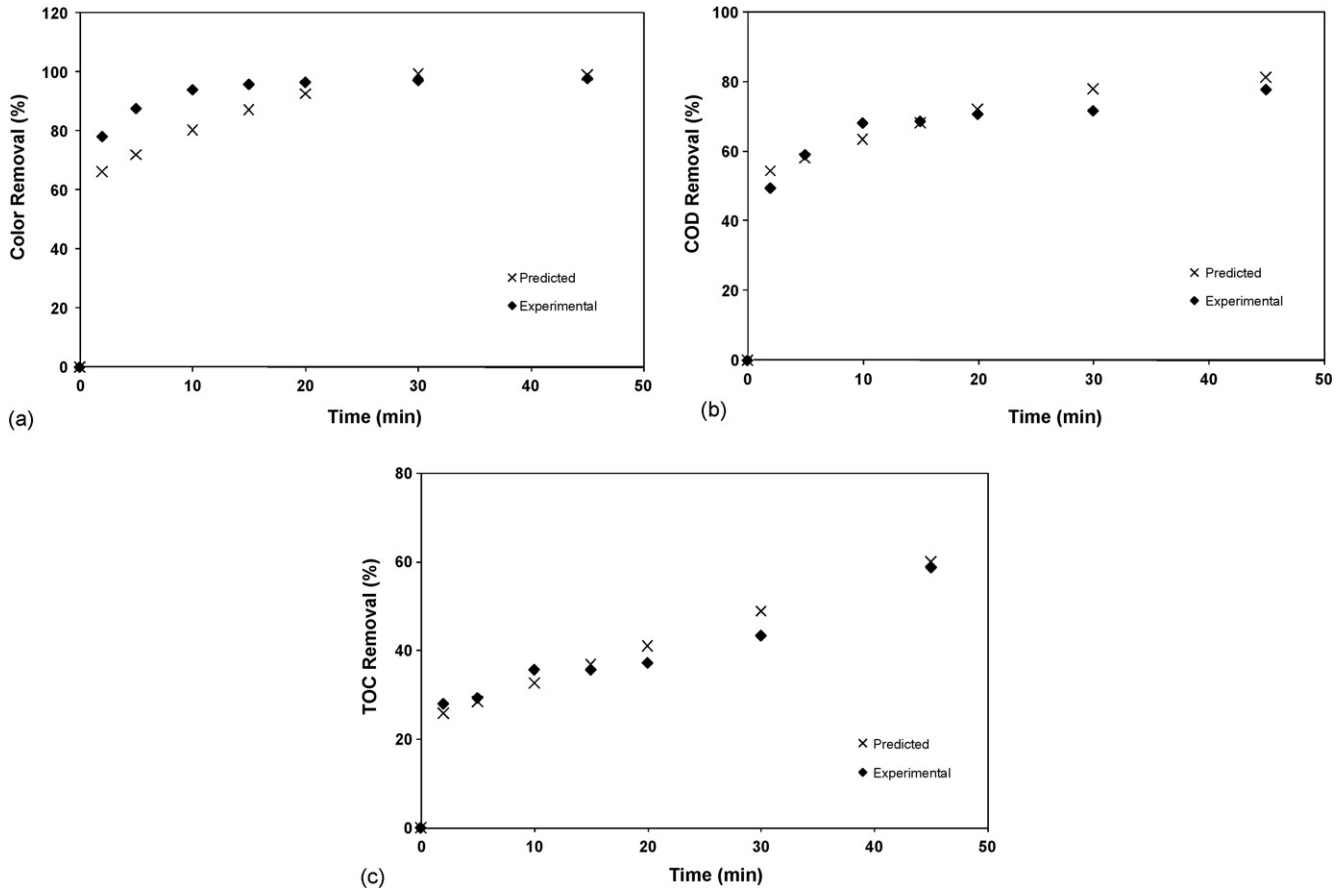

Fig. 7. Experimental and predicted percent color (a), COD (b) and TOC (c) removal efficiencies observed for synthetic Acid Blue 193 production wastewater at COD_o = 200 mg/L, $[Fe^{3+}]_o$ = 1.5 mM; $[H_2O_2]_o$ = 35 mM; pH_o 2.8.

be raised to higher values to maintain high treatment efficiencies in terms of all selected response variables (color, COD and TOC).

3.4. Application of optimized Photo-Fenton-like treatment conditions to synthetic Acid Blue 193 production wastewater

Experimentally obtained removal efficiencies for Photo-Fenton-like treatment of synthetic Acid Blue 193 production wastewater (COD_o = 200 mg/L) were compared with the values predicted by the model to confirm the validity of the optimization procedure under the process conditions established for an initial COD of 200 mg/L. Fig. 7 gives experimentally and model-predicted changes in percent color (a), COD (b) and TOC (c) removal rates as a function of Photo-Fenton-like treatment time, under optimized working conditions.

As is evident from Fig. 7(a)–(c), actual and predicted color, COD as well as TOC removal efficiencies were rather close to each other, implying that the removal efficiencies estimated by the empirical model were quite well validated by the experimentally obtained results. For instance, experimentally observed and modeled percent removal efficiencies obtained after 45 min Photo-Fenton-like treatment under optimized working conditions were found as 98 and 99%, 78 and 81%, 59 and 60% in terms color, COD and TOC parameters, respectively. Experimental findings for color, COD and TOC abatement rates revealed that by RSM-based process optimization using CCD, it was possible to save considerable time and effort for the estimation of optimum working conditions to achieve highest treatment efficiencies.

3.5. Model verification on Photo-Fenton-like oxidation of synthetic and real Reactive Black 39 production wastewater

Synthetic and real RB 39 production wastewaters were also subjected to Photo-Fenton-like treatment under optimum working conditions determined for acid dye (AB 193) production wastewater. In this way, the validity of the RSM-predicted process optimums could be verified by applying the empirical model for Photo-Fenton-like treatment of different and real azo dye production effluents. As aforementioned, the optimum working conditions were established as Fe^{3+} = 1.5 mM, H_2O_2 = 35 mM and t_r = 45 min for effluents having a COD in the range of 150–200 mg/L. RSM-predicted and experimentally obtained treatment efficiencies (response variables) under these conditions were summarized in Table 6 for real and synthetic RB 39 production wastewater.

As can be seen from Table 6, in the case of synthetic RB 39 production wastewater, experimentally achieved percent color and COD removal (100 and 84%, respectively) were slightly higher than those foreseen by the empirical model, namely 99% color and 82% COD removals. These slight discrepancies are speculatively due to the differences in molecular structures of AB 193 and RB 39 and/or their concentrations in the synthetic dye production wastewater. On the other hand, TOC removal efficiencies experimentally obtained for synthetic RB 39 production wastewater were appreciably lower (53%) as compared with the model prediction (61%) for its initial COD content, indicating that the complete mineralization of RB 39 production effluent is a harder task than that of AB 193 production effluent as a consequence

Table 6
Model-predicted and experimentally obtained percent color, COD and TOC removal efficiencies obtained for Photo-Fenton-like treatment of synthetic and real RB 39 production effluent under optimized working conditions (Fe^{3+} = 1.5 mM; H_2O_2 = 35 mM; t_r = 45 min).

Responses	Synthetic RB 39 production wastewater (COD_o = 195 mg/L)		Real RB 39 production wastewater (COD_o = 165 mg/L)	
	Model	Experimental	Model	Experimental
Color removal (%)	99	100	100	100
COD removal (%)	82	84	84	69
TOC removal (%)	61	53	70	37
DF[a]	0.85	–	0.94	–

[a] Desirability factor.

again of differences in molecular structure and/or composition as well as type and quantity of intermediate advanced oxidation products.

In case of real RB 39 production effluent (COD_o = 165 mg/L), although 100% decolorization was experimentally achieved within the treatment time (t_r = 45 min) anticipated by the model, a significant retardation occurred as compared to the color abatement rate of the synthetic RB 39 production wastewater, as can be seen from Fig. 8 presenting changes in color, COD and TOC removals during Photo-Fenton-like treatment of synthetic and real RB 193 production effluent. Moreover, experimentally achieved percent COD and TOC removal rates were found considerably lower than estimated by the model predictions, as is evident in Table 6 and Fig. 8(b) and (c).

The significant decrease in treatment efficiency observed for real RB 39 production wastewater was attributable to its high Cl^- concentration (3500 mg/L) as compared to that of the synthetic azo dye production wastewaters (see characterization Table 1 for comparison). It has been reported in former studies Cl^- react with $^\bullet OH$ under acidic pH conditions thus acting as strong free radical scavengers [44] dramatically retarding the oxidation rate and efficiency of advanced oxidation processes as given in reaction (8):

$$Cl^- + {}^\bullet OH \rightarrow ClOH^{\bullet -} \quad k_{^\bullet OH,Cl^-} = 3.0 \times 10^9 (M^{-1}\,s^{-1}) (\text{at pH 2–3}) \tag{9}$$

In addition, former studies have also postulated that when more than 0.1 M Cl^- ion is added to the Photo-assisted Fenton reaction at pH 2–3, UV-photolysis of in situ formed $FeCl^{2+}$ complexes occur that effectively compete with $Fe(OH)^{2+}$ complexes for UV-A light and hence decrease the $^\bullet OH$ production rate [45]:

$$Fe^{3+} + Cl^- \leftrightarrow FeCl^{2+} \quad K = 5.34\,M^{-1} \tag{10}$$

$$FeCl^{2+} + h\upsilon \rightarrow Fe^{2+} + Cl^\bullet \quad \phi \text{ at } 347\,nm = 0.5 \tag{11}$$

$$Cl^\bullet + Cl^- \rightarrow Cl_2^{\bullet -} \quad k_1 = 2 \times 10^{10}\,M^{-1}\,s^{-1} \tag{12}$$

The radical species $Cl^\bullet/Cl_2^{\bullet -}$ rapidly undergo undesired chlorination reactions with organic compounds (R) leading to the formation of potentially toxic and/or carcinogenic RCl (also known

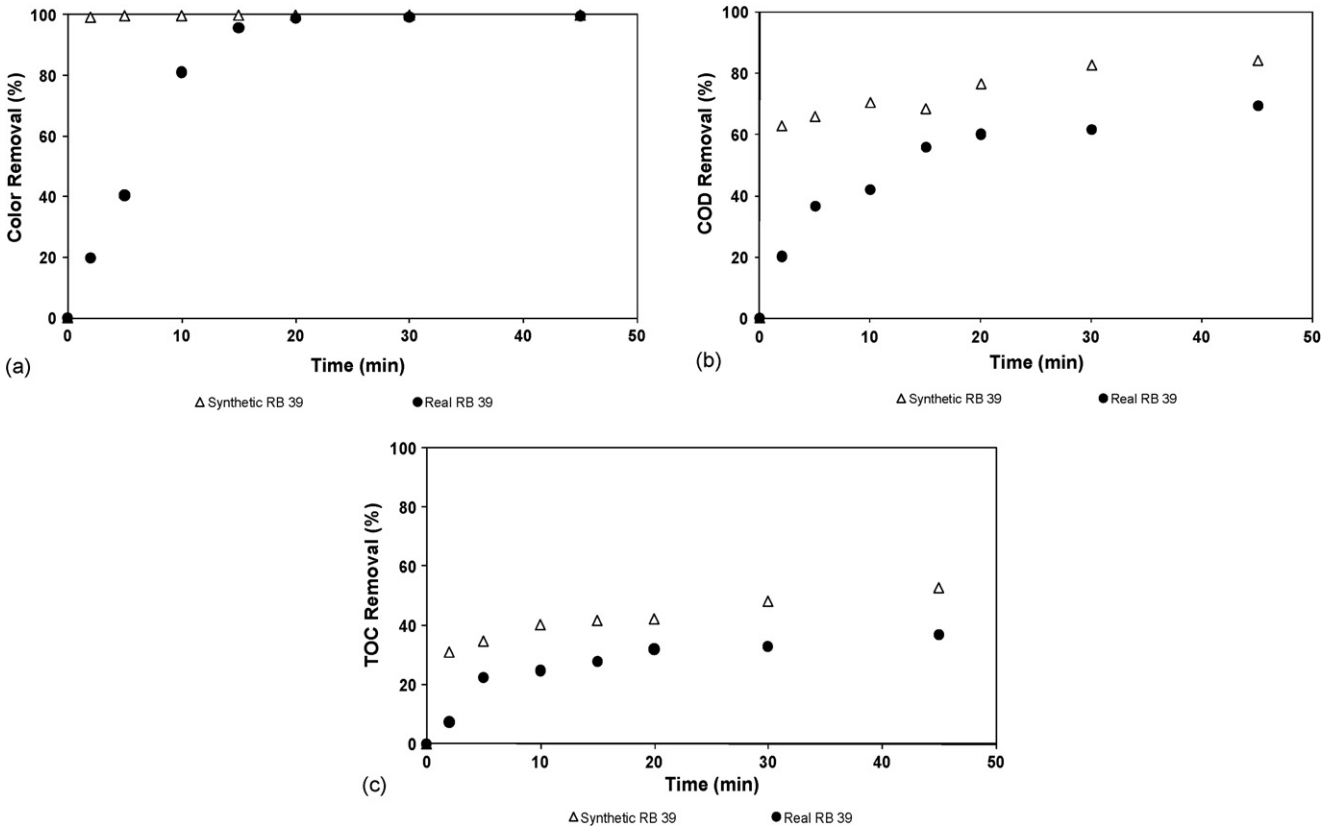

Fig. 8. Time-dependent changes in percent color (a), COD (b) and TOC (c) removal efficiencies experimentally obtained for synthetic (COD_o = 195 mg/L) and real (COD_o = 165 mg/L) RB 39 production effluents during Photo-Fenton-like treatment. Experimental conditions: $[Fe^{3+}]_o$ = 1.5 mM; $[H_2O_2]_o$ = 35 mM; pH_o = 2.8.

as adsorbable organic halogens; AOX) [45];

$$R + Cl^{\bullet}/Cl_2^{\bullet -} \rightarrow RCl \quad k_2 = 3.7 \times 10^7\ M^{-1}\ s^{-1}$$
$$\text{Acid Orange 7 (Orange II)} \qquad (13)$$

On the other hand, $Cl^{\bullet}/Cl_2^{\bullet -}$ also consume H_2O_2 to form the less powerful free radical $HO_2^{\bullet}$ [45];

$$Cl^{\bullet} + H_2O_2 \rightarrow HO_2^{\bullet} + Cl^- + H^+ \quad k_3 = 1 \times 10^9\ M^{-1}\ s^{-1} \qquad (14)$$

$$Cl_2^{\bullet -} + H_2O_2 \rightarrow HO_2^{\bullet} + 2Cl^- + H^+ \quad k_4 = 9 \times 10^4\ M^{-1}\ s^{-1} \qquad (15)$$

The above given side reactions delineate that the Photo-Fenton-like treatment of industrial effluents with high chloride content in not only relatively less efficient but also less attractive from the environmental point of view.

4. Conclusions

The present experimental study aimed at investigating the treatability of azo dye production wastewaters via Photo-Fenton-like advanced oxidation process under varying working conditions. For this purpose, synthetic Acid Blue 193 and Reactive Black 39 production wastewaters from the synthesis reactor rinsing stage as well as real Reactive Black 39 production wastewater from the reverse osmosis purification stage of the azo dye manufacturing process were selected as model effluents. Response surface methodology was applied to assess the individual and interactive effects of several critical process parameters on decolorization and organic carbon (COD and TOC) abatement rates and to optimize the Photo-Fenton-like treatment process. The model polynomial functions derived from the experimental data expressed the empirical relationship between the independent, manipulating process variables (Fe^{3+}, H_2O_2 concentrations, initial COD and reaction time) and responses (color, COD and TOC removals) for Photo-Fenton-like treatment of Acid Blue 193 production effluent. The established models were also used to characterize and optimize the Photo-Fenton-like treatment of synthetic and real Reactive Black 39 production effluents. Experimental findings have revealed that Photo-Fenton-like advanced oxidation is an effective treatment method for complete decolorization accompanied with appreciable COD and TOC removals from azo dye production wastewater. The obtained results demonstrated the usefulness of response surface methodology in predicting the treatment performance of the Photo-Fenton-like process as well as the interactive effects of manipulating process variables. However, it should be kept in mind that the treatment efficiencies and kinetics may vary such that empirical models may fail to predict radical changes in effluent composition and strength. For instance, considering our experimental results it is strongly recommended to determine the chloride content of the wastewater prior to application of Photo-Fenton-like treatment, since treatment efficiency of Fe-based photochemical advanced oxidation processes might be considerably reduced in case of high chloride concentrations acting as free radical scavengers at acidic pHs.

Acknowledgements and credits

The authors are thankful to Dr. Rezzan Karaaslan (SETAS Chemical Company) for providing the chemicals used to prepare synthetic acid and reactive dye production wastewaters as well as the real reactive dye production effluent. The financial support of Istanbul Technical University Research Foundation is also appreciated.

References

[1] M. Kornaros, G. Lyberatos, Biological treatment of wastewaters from a dye manufacturing company using a trickling filter, J. Hazard. Mater. 136 (2006) 95–102.
[2] T.H. Kim, C. Park, S. Kim, Water recycling from desalination and purification process of reactive dye manufacturing industry by combined membrane filtration, J. Clean. Prod. 13 (2005) 779–786.
[3] R.D. Voyksner, R. Straub, J.T. Keever, H.S. Freeman, W.N. Hsu, Determination of aromatic amines originating from azo dyes by chemical reduction combined with liquid chromatography/mass spectrometry, Environ. Sci. Technol. 27 (1993) 1665–1672.
[4] H.Y. Shu, M.C. Chang, W.P. Hsieh, Remedy of dye manufacturing process effluent by UV/H_2O_2 process, J. Hazard. Mater. B128 (2006) 60–66.
[5] C. Gottschalk, J.A. Libra, A. Saupe, Ozonation of Water and Wastewater: A Practical Guide to Understanding Ozone and its Application, Wiley–VCH, Weinheim, New York, 2000.
[6] F.J. Beltrán, Ozone Reaction Kinetics for Water and Wastewater Systems, Lewis Publishers, Boca Raton, FL, 2004.
[7] P.A. Carneiro, R.F.P. Nogueira, M.V.B. Zanoni, Homogeneous photodegradation of C.I. Reactive Blue 4 using a photo-Fenton process under artificial and solar irradiation, Dyes Pigments 74 (2007) 127–132.
[8] Y.H. Huang, S.T. Tsai, Y.F. Huang, C.Y. Chen, Degradation of commercial azo dye Reactive Black B in photo/ferrioxalate system, J. Hazard. Mater. 140 (2007) 382–388.
[9] I. Arslan, I. Akmehmet Balcioglu, Degradation of commercial reactive dyestuffs by heterogeneous and homogeneous advanced oxidation processes: a comparative study, Dyes Pigments 43 (1999) 95–108.
[10] O. Sogut, M. Akgun, Treatment of textile wastewater by SCWO in a tube reactor, J. Supercrit. Fluids 43 (2007) 106–111.
[11] E. Chatzisymeon, N.P. Xekoukoulotakis, A. Coz, N. Kalogerakis, D. Mantzavinos, Electrochemical treatment of textile dyes and dyehouse effluents, J. Hazard. Mater. B137 (2006) 998–1007.
[12] K. Okitsu, K. Iwasaki, Y. Yobiko, H. Bandow, R. Nishimura, Y. Maeda, Sonochemical degradation of azo dyes in aqueous solution: A new heterogeneous kinetics model taking into account the local concentration of OH radicals and azo dyes, Ultrason. Sonochem. 12 (2005) 255–262.
[13] R.J. Bigda, Consider Fenton's chemistry for wastewater treatment, Chem. Eng. Prog. 91 (1995) 62–66.
[14] S.F. Kang, C.H. Liao, H.P. Hung, Peroxidation treatment of dye manufacturing wastewater in the presence of ultraviolet light and ferrous ions, J. Hazard. Mater. B65 (1999) 317–333.
[15] H.Y. Shu, W.P. Hsueh, Treatment of dye manufacturing plant effluent using an annular UV/H_2O_2 reactor with multi-UV lamps, Sep. Purif. Technol. 51 (2006) 379–386.
[16] M. Barbeni, C. Minero, E. Pelezzitti, E. Borgarrello, N. Serpone, Chemical degradation of chlorophenols with Fenton's reagent, Chemosphere 16 (1987) 2225–2237.
[17] C. Walling, Fenton's reagent revisited, Acc. Chem. Res. 8 (1975) 125–131.
[18] H.J.H. Fenton, Oxidation of tartaric acid in presence of iron, J. Chem. Soc. 65 (1894) 899.
[19] G. Ruppert, R. Bauer, G. Heisler, The Photo-Fenton reaction—an effective photochemical wastewater treatment process, J. Photochem. Photobiol. A 73 (1993) 75–78.
[20] J.J. Pignatello, Dark and photoassisted Fe^{3+} catalyzed degradation of chlorophenoxy herbicides by hydrogen peroxide, Environ. Sci. Technol. 26 (1992) 944–951.
[21] J. Jeong, J. Yoon, pH effect on OH radical production in photo/ferrioxalate system, Wat. Res. 39 (2005) 2893–2900.
[22] A. Safarzadeh-Amiri, J.R. Bolton, S.R. Cater, Ferrioxalate-mediated photodegradation of organic pollutants in contaminated water, Wat. Res. 31 (1997) 787–798.
[23] A. Safarzadeh-Amiri, J.R. Bolton, S.R. Cater, The use of iron in advanced oxidation processes, J. Advan. Oxid. Technol. 1 (1996) 18–26.
[24] M.A. Alim, J.H. Lee, C.C. Akoh, M.S. Choi, M.S. Jeon, J.A. Shin, K.T. Lee, Enzymatic transesterification of fractionated rice bran oil with conjugated linoleic acid: optimization by response surface methodology, LWT-Food Sci. Technol. 41 (2008) 764–770.
[25] R.H. Myers, D.C. Montgomery, Response Surface Methodology: Process and Product Optimization using Designed Experiments, 2nd ed., John Wiley & Sons, USA, 2002.
[26] J.M. Monteagudo, A. Durán, C. López-Almodóvar, Homogeneus ferrioxalate-assisted solar Photo-Fenton degradation of Orange II aqueous solutions, Appl. Catal. B 83 (2008) 46–55.
[27] A. Aleboyeh, N. Daneshvar, M.B. Kasiri, Optimization of C.I. Acid Red 14 azo dye removal by electrocoagulation batch process with response surface methodology, Chem. Eng. Process. 47 (2008) 827–832.
[28] M. Sleiman, D. Vildozo, C. Ferronato, J.M. Chovelon, Photocatalytic degradation of azo dye Metanil Yellow: optimization and kinetic modeling using a chemometric approach, Appl. Catal. B Environ. 77 (2007) 1–11.
[29] M.S. Secula, G.D. Suditu, I. Poulios, C. Cojocaru, I. Cretescu, Response surface optimization of the photocatalytic decolorization of a simulated dyestuff effluent, Chem. Eng. J. 141 (2008) 18–26.
[30] B.K. Korbahti, Response surface optimization of electrochemical treatment of textile dye wastewater, J. Hazard. Mater. 145 (2007) 277–286.
[31] M. Muthukumar, D. Sargunamani, N. Selvakumar, J.V. Rao, Optimisation of ozone treatment for colour and COD removal of acid dye effluent

using central composite design experiment, Dyes Pigments 63 (2004) 127–134.
[32] C.G. Hatchard, C.A. Parker, A new sensitive chemical actinometer. II. Potassium ferrioxalate as a standard chemical actinometer, Proc. R. Soc. Lond. A235 (1956) 518–536.
[33] ISO 6060. Water quality-determination of the chemical oxygen demand, ISO 6060/TC 147: 2nd ed. Geneva, 1989.
[34] Deutsche Normen. Summarische Wirkungs-und Stoffkenngrößen (Gruppe H), Bestimmung des Chemischen Sauerstoffbedarfs (CSB) im Bereich über 15 mg/L (H41), DIN 38 409 H 41-2, 1980.
[35] APHA-AWWA-WPCF, Standard Methods for the Examination of Water and Wastewater, 21st ed., Amer. Public Health Assoc., Washington, DC, 2005.
[36] D. Bas, I.H. Boyaci, Modeling and optimization. I. Usability of response surface methodology, J. Food Eng. 78 (2007) 836–845.
[37] H. Ceylan, S. Kubilay, N. Aktas, N. Sahiner, An approach for prediction of optimum reaction conditions for laccase-catalyzed bio-transformation of 1-naphthol by response surface methodology (RSM), Bioresour. Technol. 99 (2008) 2025–2031.
[38] I.H. Cho, K.D. Zoh, Photocatalytic degradation of azo dye (Reactive Red 120) in TiO_2/UV system: optimization and modeling using a response surface methodology (RSM) based on the central composite design, Dyes Pigments 75 (2007) 533–543.
[39] Design-Expert Software Trial Version 6.0.7, User's Guide, 2008.
[40] W.Z. Tang, C.P. Huang, 2,4-Dichlorophenol oxidation by Fenton's reagent, Environ. Technol. 17 (1996) 1373–1378.
[41] J.A. Giroto, R. Guardani, A.C.S.C. Teixeira, C.A.O. Nascimento, Study on the Photo-Fenton degradation of polyvinyl alcohol in aqueous solution, Chem. Eng. Process. 45 (2006) 523–532.
[42] I.A. Balcioglu, I. Arslan, Partial oxidation of reactive dyestuffs and synthetic textile dye-bath by the O_3 and O_3/H_2O_2 processes, Water Sci. Technol. 43 (2001) 221–228.
[43] G.V. Buxton, C.L. Greenstock, W.P. Helman, A.B. Ross, Critical review of rate constants for reactions of hydrated electrons, hydrogen atoms and hydroxyl radicals in aqueous solution, J. Phys. Chem. Ref. Data 17 (1988) 513–886.
[44] A.E. Grigor'ev, I.E. Makarov, A.K. Pikaev, Formation of $Cl_2^{\bullet-}$ in the bulk solution during the radiolysis of concentrated aqueous solutions of chlorides, High Energy Chem. 21 (1987) 99–102.
[45] J. Kiwi, A. Lopez, V. Nadtochenko, Mechanism and kinetics of the $OH^{\bullet-}$ radicals intervention during Fenton oxidation in the presence of a significant amount of radical scavenger (Cl^-), Environ. Sci. Technol. 34 (2000) 2162–2168.